Research Paper

Mapping glutathione utilization in the developing zebrafish (*Danio rerio*) embryo

Archit Rastogi[a], Christopher W. Clark[b], Sarah M. Conlin[b], Sarah E. Brown[b],
Alicia R. Timme-Laragy[a,b,*]

[a] *Molecular & Cellular Biology Graduate Program, University of Massachusetts, Amherst, MA, 01003, USA*
[b] *Department of Environmental Health Sciences, School of Public Health and Health Sciences, University of Massachusetts, Amherst, MA, 01003, USA*

A B S T R A C T

Glutathione (GSH), the most abundant vertebrate endogenous redox buffer, plays key roles in organogenesis and embryonic development, however, organ-specific GSH utilization during development remains understudied. Monochlorobimane (MCB), a dye conjugated with GSH by glutathione-s-transferase (GST) to form a fluorescent adduct, was used to visualize organ-specific GSH utilization in live developing zebrafish (*Danio rerio*) embryos. Embryos were incubated in 20 μM MCB for 1 h and imaged on an epifluorescence microscope. GSH conjugation with MCB was high during early organogenesis, decreasing as embryos aged. The heart had fluorescence 21-fold above autofluorescence at 24 hpf, dropping to 8.5-fold by 48 hpf; this increased again by 72 hpf to 23.5-fold, and stayed high till 96 hpf (18-fold). The brain had lower fluorescence (10-fold) at 24 and 48 hpf, steadily increasing to 30-fold by 96 hpf. The sensitivity and specificity of MCB staining was then tested with known GSH modulators. A 10-min treatment at 48 hpf with 750 μM *tert*-butylhydroperoxide, caused organ-specific reductions in staining, with the heart losing 30% fluorescence, and, the brain ventricle losing 47% fluorescence. A 24 h treatment from 24-48 hpf with 100 μM of N-Acetylcysteine (NAC) resulted in significantly increased fluorescence, with the brain ventricle and heart showing 312% and 240% increases respectively, these were abolished upon co-treatment with 5 μM BSO, an inhibitor of the enzyme that utilizes NAC to synthesize GSH. A 60 min 100 μM treatment with ethacrynic acid, a specific GST inhibitor, caused 30% reduction in fluorescence across all measured structures. MCB staining was then applied to test for GSH disruptions caused by the toxicants perfluorooctanesulfonic acid and mono-(2-ethyl-hexyl)phthalate; MCB fluorescence responded in a dose, structure and age-dependent manner. MCB staining is a robust, sensitive method to detect spatiotemporal changes in GSH utilization, and, can be applied to identify sensitive target tissues of toxicants.

1. Introduction

Endogenous redox signaling has important ramifications for cell fate decisions and organogenesis during embryonic development, with precise regulatory mechanisms having evolved to permit redox signaling pathways to proceed; a loss of control over these pathways results in oxidative stress [1–5]. The most abundant endogenous redox buffer in vertebrates is the small thiol, glutathione – a tripeptide of glutamate, cysteine and glycine. Reduced glutathione (GSH) can neutralize redox disruptors by serving as an electron donor and forming a disulfide bond either with itself, or, with other molecules. Oxidized glutathione (GSSG), a homodimer of GSH can be recycled back to its reduced form in a reaction catalyzed by glutathione reductase (GR) [6–8]. The ratio of oxidized to reduced glutathione concentrations

([GSSG]/[GSH]) can be incorporated into the Nernst equation to arrive at the cellular redox potential (E_h), reported in mV [9]. The GSH E_h of the developing embryo is highly dynamic, yet tightly regulated, with interruptions leading to early differentiation, altered cell migration patterns, apoptosis and changes in embryo polarity [10–12].

Relatively small changes in the GSH E_h can have significant biological consequences. For example, a 12–16 mV oxidation of the total cellular GSH pool is sufficient to increase GST activity 2–3 fold, resulting in increased differentiation of human adenocarcinoma cells into enterocytes [13]. In general, the GSH E_h becomes increasingly oxidized as cells grow and differentiate. CaCo-2 cells show a 40 mV oxidation in the GSH E_h as they approach contact inhibition; this change is restricted to the GSH redox couple, with no observable change in the thioredoxin system – another key vertebrate redox buffer [14]. Typically, the GSH/

GSSH couple E_h ranges from -260 to -150 mV in living systems, with disruptions in the E_h impacting signal transduction, protein function, and cell cycle regulation [9,15].

Many environmental toxicants are potent exogenous disruptors of the GSH E_h [16]. This disruption can be a direct result of GSH depletion as part of the Phase II metabolism of these xenobiotics; alternately, these chemicals can undergo a reduction to generate a product that can react with oxygen to regenerate the parent compound, thereby entering a redox cycle. These reactions consume cellular reducing agents like NADPH and produce large amounts of reactive oxygen species (ROS) as byproducts, shifting the GSH E_h from being largely reducing to more oxidizing [17]. Xenobiotics can also activate the Nuclear Factor Erythroid-2 (Nrf2) transcription factor, which coordinates cellular antioxidant defense machinery [18–22]. This can be through direct interactions with Nrf2, or, due to changes in the GSH E_h. Nrf2 translocates to the nucleus and activates the transcription of the Nrf2 gene battery, which include GSH synthesis genes, and, the Glutathione-S-Transferase (GST) enzyme superfamily [23]. GSTs conjugate GSH to xenobiotics; these GS-conjugates can often be readily excreted, providing living systems with an efficient method to combat toxic insults. GST expression however, is highly spatiotemporally divergent in vertebrates, leading to differential susceptibilities and sensitivities of organ systems during development [24–27]. Furthermore, disruptions in the GSH E_h during organogenesis cause altered glutathionylation of spliceosome related proteins leading to dysregulation of normal signaling in rat fetuses; these alterations occur to different degrees in different
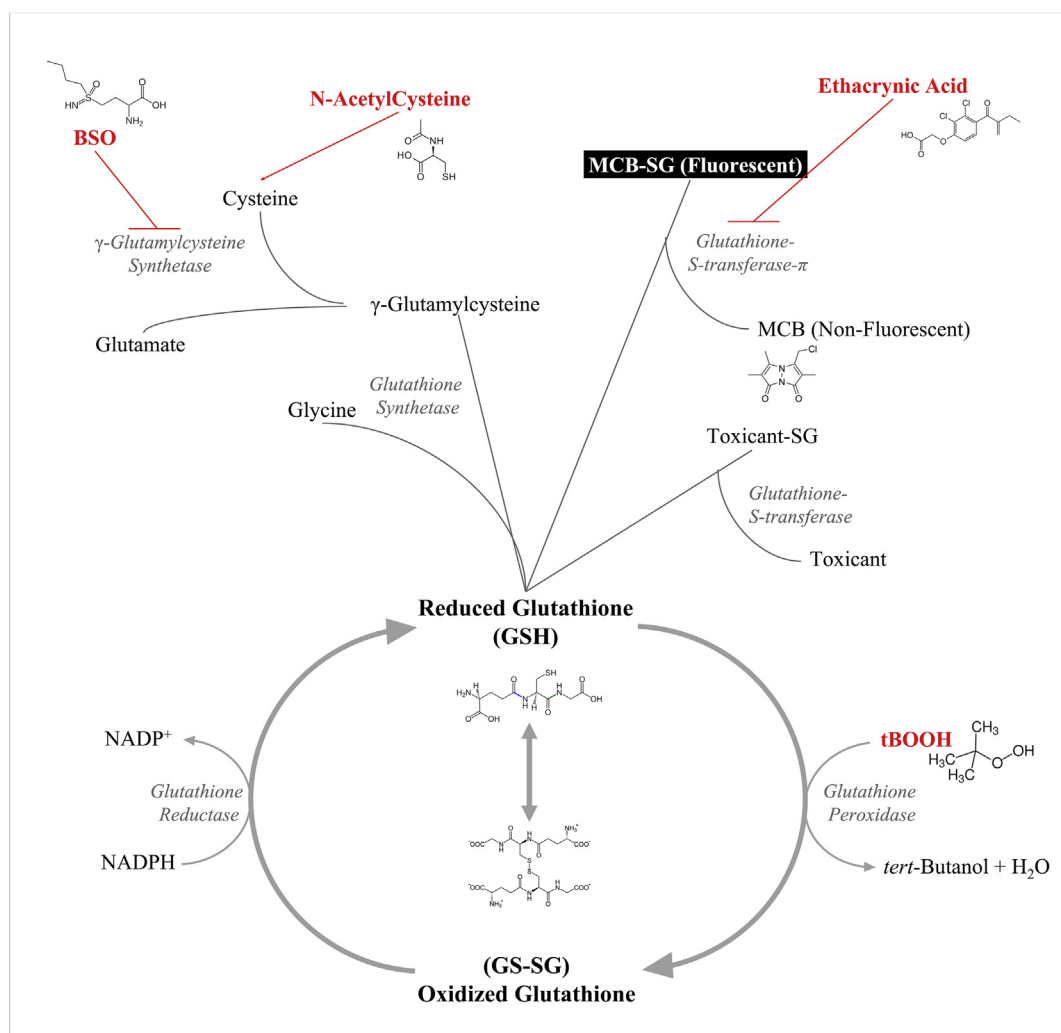

Fig. 1. The glutathione cycle and modulating factors. The glutathione cycle. Grey italicized text represents names of enzymes involved in the pathway. All the treatments done are highlighted in red. The fluorescent GS-MCB adduct is highlighted in white. (For interpretation of the references to colour in this figure legend, the reader is referred to the Web version of this article.)

embryonic compartments, underscoring the need to better characterize spatiotemporal glutathione redox dynamics during embryogenesis [28].

Zebrafish are a widely used model for embryonic development, owing to their low cost, external development, transparent embryos, high fecundity and accelerated growth when contrasted with conventional mammalian models [29,30]. The zebrafish model is also finding broad application in the field of developmental toxicology, with a steady increase in the number of studies utilizing zebrafish for the risk and safety assessment of chemical exposures [31,32]. In zebrafish embryos, the GSH E_h changes specifically and directionally during development, in a pattern similar to that seen in developing mouse embryos [33,34].

The ability of the GSH system to respond and recover from oxidizing conditions changes with developmental stage. Zebrafish embryos are increasingly resistant to oxidizing exposures from 18 h post fertilization (hpf) (when the majority of the endoderm derived organs start developing) -72 hpf (most major endoderm-derived organs have developed and the embryo hatches); after hatching, embryos become much more sensitive to pro-oxidant exposures [35]. This is in keeping with changes in the concentration of GSH in zebrafish embryos during development, which nearly doubles between 24 to 36 hpf [33]. A similar trajectory for the GSH E_h has been reported in cultured mouse embryos [28]. GSH synthesis has also been demonstrated to be essential for mammalian embryonic development, with mouse embryos lacking a functional enzyme to synthesize GSH failing to gastrulate and aborting before reaching the 8–12 somite stage [36,37].

Although total GSH concentrations and overall GSH E_h during early embryogenesis are well reported, data regarding the spatial distribution of GSH during embryonic development are limited. This is a critical gap in knowledge, since different organs develop in their own redox microenvironment, and hypothetically, are differentially affected by the aforementioned redox disruptions. This gap has arisen, in part, due to few suitable methods for the visualization of GSH redox dynamics in live animals. The use of genetically encoded fluorescent redox sensors, especially roGFP to monitor physiological GSH E_h has been steadily increasing [38]. In the zebrafish, roGFP has been used to monitor the effects of biliary toxins on the GSH concentration of the developing liver, and, GSH E_h responses of developing cardiomyocytes and enterocytes to prooxidant challenges [39,40]. Although these transgenic models provide a useful tool to test *a priori* hypotheses regarding the organ-specific toxicity of xenobiotics, there is a need for unbiased, whole organism-level data about GSH redox dynamics, particularly in the context of the identifying sensitive target organs in developmental toxicity studies. Fluorescent dyes are amongst the most feasible options to measure redox dynamics at a whole-organism level. These primarily include dyes that label ROS like dichlorofluorescein diacetate (DCF-DA), or, dyes that label GSH like halogenated bimanes [41,42].

Monochlorobimane (MCB), a cell-permeable non fluorescent bimane dye, is conjugated to GSH by GST forming a fluorescent adduct in living systems [43]. Thus, fluorescence intensity of MCB serves as a good proxy for the rate of glutathione utilization [42]. Historically, MCB has been used predominantly in cell culture studies to determine glutathione compartmentalization and changes associated with diverse processes including but not limited to cell growth, differentiation, xenobiotic metabolism and, oocyte maturation [44–46]. Previous studies have compared various small thiol dyes and found that MCB displays greater specificity for GSH than other thiol dyes [47,48]. In the zebrafish, the Gst isozyme superfamily has been well-characterized both during development and in adult fish [24]. MCB is known to be a substrate for all the known zebrafish GST isozymes, with Gstτ1a having the lowest affinity and Gstπ1 having the highest affinity [49].

In this study, we investigate the suitability *in vivo* staining of zebrafish embryos with MCB to visualize tissue-specific glutathione utilization. We confirm the specificity and sensitivity of MCB as a reliable tool to measure changes in glutathione utilization using well-characterized modulators of the glutathione pathway in a live animal

(Fig. 1). Finally, we applied this method to detect spatial changes in GSH homeostasis upon exposure to the environmental contaminants perfluorooctanesulfonic acid (PFOS) and mono(2-ethylhexyl) phthalate (MEHP), as an illustration of its application potential.

2. Material and methods

2.1. Chemicals and reagents

Monochlorobimane (Catalog #M13813MP) was purchased from Molecular Probes (Eugene, OR, USA). Dimethyl Sulfoxide (DMSO; Catalog #BP231-1) was purchased from Fisher Scientific (Pittsburgh, PA, USA). *Tert*-Butyl hydroperoxide (tBOOH; Catalog #A13926AP) and *N*-acetyl-L-cysteine (NAC; Catalog #A1540914) were purchased from Alfa Aesar (Ward Hill, MA, USA). Ethacrynic Acid (ETA; Catalog #BMLEI1280001) and L-Buthionine-(S,R)-sulfoximine (BSO; Catalog #BML-FR117-0500) were purchased from Enzo Life Sciences (Farmingdale, NY, USA). Potassium perfluorooctane sulfonate (PFOS; Catalog #33829) was purchased from Millipore-Sigma (Burlington, MA, USA). Mono(2-ethylhexyl) phthalate (MEHP; Catalog #ALR-138S–CN) was purchased from AccuStandard (New Haven, CT, USA).

2.2. Fish husbandry and embryo sampling

Homozygous *mitfa($^{b692/b692}$)* mutant zebrafish (*Danio rerio*) crossed on the *AB* wild type strain were used for all experiments. This line was chosen as these mutants fail to develop melanocytes and display an albinism phenotype thereby eliminating pigment that would otherwise occlude imaging. Adult fish were maintained on an automated Aquaneering (San Diego, CA, USA) system in accordance with the Guide for the Care and the Use of Laboratory Animals of the National Institutes of Health and with approval from the University of Massachusetts Amherst Institutional Animal Care and Use Committee (Animal Welfare Assurance Number A3551-01). The fish were housed at 28.5 °C on a 14 h light, 10 hdark cycle in, and fed GEMMA Micro 300 (Skretting, Westbrook, ME, USA) twice daily. Large breeding tanks were setup with approximately 20 adult female and 10 adult male fish. Embryos were collected 1 h post fertilization, washed and screened for fertilization status and staged according to Kimmel et al. [50]. The embryos were dechorionated at 24 hpf and reared in borosilicate glass scintillation vials with 1 ml 0.3x Danieau's per embryo.

2.3. Glutathione modulating exposures

Embryos aged 48 hpf were exposed to 750 μM tBOOH, stock prepared in water, for 10 or 30 min, the tBOOH was washed out immediately prior to MCB staining. Embryos were exposed to either 100 μM NAC, 5 μM BSO, or, a combination of the two from 24 to 48 hpf. These concentrations were chosen based on previous studies in zebrafish embryos [51,52]. The NAC and BSO stocks were prepared in 0.3x Danieau's. The embryos were MCB stained and imaged at 48 hpf. Embryos aged 48 hpf were exposed to 100 μM ETA (0.1% DMSO) for 30 min or 1 h immediately prior to MCB staining and imaging. Embryos aged 48 hpf were exposed to 10 μM Menadione (0.01% DMSO) for 1 h immediately prior to MCB staining and imaging. All embryos were manually dechorionated at 24 hpf using fine watchmaker's forceps and reared, exposed and stained in 20 ml borosilicate glass scintillation vials with 1 ml 0.3x Danieau's per embryo.

2.4. Toxicant exposures

Embryos were exposed to 3.2 μM or 32 μM PFOS (0.01% DMSO),or, 200 μg/L MEHP (0.01% DMSO) starting at 3 hpf. The PFOS and MEHP concentrations were chosen based on previous studies which established that these doses produce sub-lethal effects in zebrafish embryos, with no gross malformations [18,53–55]. The dosing solutions were

refreshed daily; embryos were manually dechorionated at 24 hpf and reared, exposed and stained in 20 ml borosilicate glass scintillation vials with 1 ml 0.3x Danieau's per embryo. The embryos were imaged at 48 hpf and 72 hpf, with exposures terminated immediately prior to MCB staining and imaging.

2.5. Monochlorobimane staining, imaging and data analysis

Pools of ten dechorionated embryos were placed in 3 ml 0.3x Danieau's in glass scintillation vials and stained with 20 μM MCB (final DMSO conc. 0.1%) for 1 h. The embryos were then immobilized on ice for 2 min, washed with fresh Danieau's for 2 min and imaged using an inverted fluorescence microscope (EVOS FL Auto, Life Technologies, Pittsburgh, PA, USA) equipped with a DAPI filter set. In our hands, anaesthetizing embryos with MS-222 produced inconsistent, irreproducible staining patterns. This could be due to MS-222's action on Ca^{2+} release channels, and, the many interactions between Ca^{2+} and the GSH system [56]. Embryos were mounted in drops of 3% methylcellulose on glass slides and oriented laterally; we found that MCB stained plastic dishes and pipettes, causing increased levels of background fluorescence. To account for the inverted microscopy, all images presented here are mirror flipped to represent the actual orientation of the embryos. Heat-maps were generated using the 16Colors LUT in ImageJ. All image analysis was done using the EVOS FL Auto software. Briefly, freehand outlines of the specific structures were traced, and, their mean fluorescence intensity recorded, all images were blinded before analysis. All images were corrected for background and auto fluorescence.

2.6. Statistical analysis

All experiments were carried out to conform to OECD guidelines, with a minimum of two independent experimental repeats [57]. A one-way ANOVA followed by a Tukey-Kramer post-hoc test with a confidence interval of 95% was used to determine statistically significant differences between treatment groups and structures; the statistical software JMP Pro 13 was used for all analyses. We attributed the slight differences staining in control embryos to inter-clutch variability. To better control for this, a DMSO treated or untreated control group was used in every single experimental repeat; all structures were normalized to the mean yolk fluorescence of this group within each experimental repeat before the data were combined for statistical analyses.

3. Results

3.1. Glutathione utilization is highly spatiotemporal in the developing zebrafish embryo

To determine the suitability of *in vivo* MCB staining to identify spatiotemporal changes in GSH utilization in the developing embryo, zebrafish embryos were stained with MCB for 1 h and imaged at 24, 48, 72 and 96 hpf. These timepoints were chosen because they correspond to organogenesis, pharyngulation, hatching and larval stages; they have also been identified as important timepoints for investigating developmental toxicity in the zebrafish model by the OECD [57]. By 96 hpf most organs have developed and the eleutheroembryos are free-swimming; zebrafish embryos exhaust their yolk and start feeding at 7 dpf, and, are considered larvae at this age.

Fluorescence patterns in embryonic structures differed significantly at each timepoint (Fig. 2), with the gut, heart and brain demonstrating the highest fluorescence. Of the structures measured, the heart and the brain had the most dynamic fluorescence patterns. The heart had a fluorescence that was 21-fold above autofluorescence ($p < 0.0001$) at 24 hpf, dropping to 8.5-fold by 48 hpf ($p < 0.0001$); the fluorescence increased again by 72 hpf to 23.5-fold ($p < 0.0001$), and stayed high till 96 hpf (18-fold; p). The values are expressed as fold autofluorescence to account for the inherently high autofluorescence seen in certain structures in the zebrafish embryo (Supp. Fig. S1). The brain had lower fluorescence (10-fold, $p < 0.0001$) at 24 and 48 hpf, this steadily increased, doubling to 20-fold ($p < 0.0001$) at 72 hpf and increasing to 30-fold ($p < 0.0001$) at 96 hpf. The other structures measured showed higher fluorescence levels of 10-fold ($p < 0.0001$) at 24 hpf, with these levels decreasing as the embryos got older. Raw fluorescence values are tabulated in Supplementary Table T1 (Supp. Table T1).
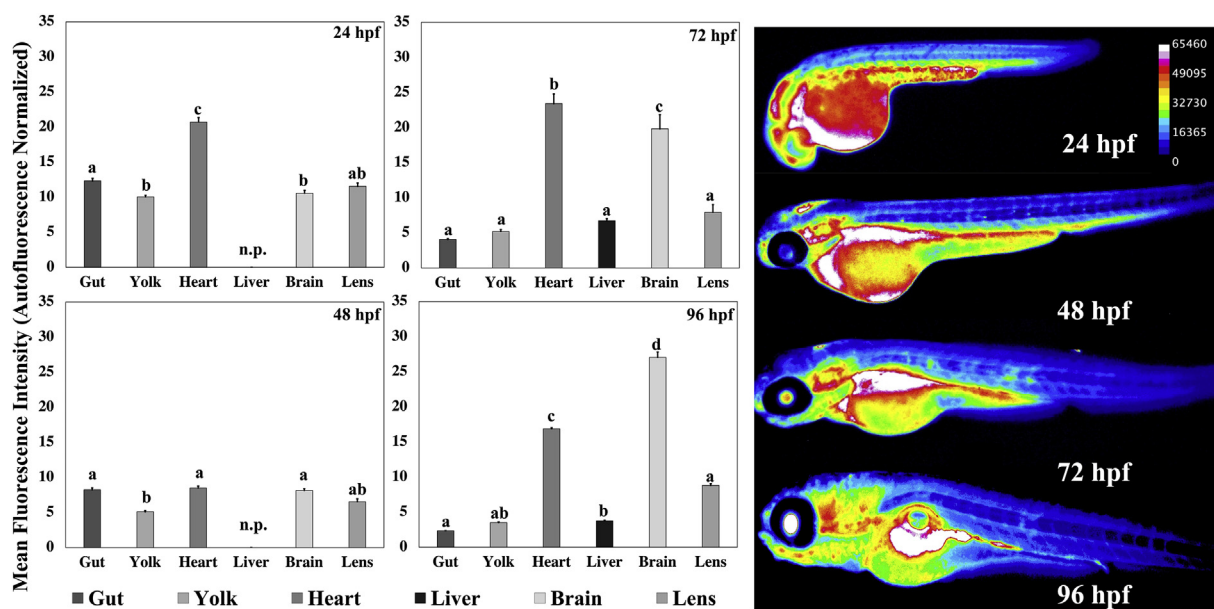

Fig. 2. Glutathione utilization is highly spatiotemporal during embryonic development. Zebrafish embryos aged 24 (n = 16), 48 (n = 27), 72 (n = 29) and 96 (n = 27) hpf were stained with MCB and imaged. Values are mean + SEM fluorescence intensities normalized to the autofluorescence intensity of the specified structure in unstained embryos. Different letters indicate statistically significant differences (p ≤ 0.05), as determined by a one-way ANOVA followed by a Tukey-Kramer post-hoc. Right: Heatmaps of MCB fluorescence at the specified ages. For raw, unprocessed images and autofluorescence images, please refer to Supp. Fig. 1.

3.2. MCB conjugation is glutathione-s-transferase mediated in live, developing zebrafish embryos

To determine that MCB conjugation was Gst mediated in zebrafish embryos, and consequently, representative of the glutathione utilization, we treated 48 hpf embryos with 100 μM ethacrynic acid (ETA) for 30 min or 1 h prior to MCB staining and imaging. ETA is a specific Gstπ inhibitor; Gstπ is the predominant isozyme in zebrafish at these early embryonic stages, with two paralogs Gstπ1 & Gstπ2 [24,49]. A 30-min treatment with ETA was insufficient to cause any significant changes in glutathione utilization across all measured structures (Supp. Fig. S2.); however a 1 h ETA treatment caused a significant decrease compared to DMSO controls of approximately 30% (p < 0.0001) in MCB fluorescence in all structures measured, with exception of the brain ventricle and the 12th somite which did not change (Fig. 3); the 12th somite was chosen as being representative of the muscular tissue. An important thing to note here is that these control embryos were treated with 0.1% DMSO, which caused a significant decrease in glutathione utilization as compared to untreated embryos and embryos treated with 0.01% DMSO (Supp. Fig. S3). Owing to ETA's inherent physical properties and low solubility in DMSO, we were unable to lower the final DMSO concentration below 0.1% in these experiments.

3.3. Monochlorobimane responds robustly to GSH modulation in the zebrafish embryo

In order to establish the sensitivity of MCB to changes in glutathione concentration, we employed the glutathione modulators NAC and BSO. NAC readily enters living cells and is deacetylated by cellular esterases thereby generating cysteine, the rate-limiting constituent of glutathione. BSO is an irreversible inhibitor of γ-glutamylcysteine synthetase, the enzyme that catalyzes the conjugation of cysteine and glutamate to generate γ-glutamylcysteine, a precursor of glutathione (Fig. 4). We treated zebrafish embryos for 24 h with either 100 μM NAC, 5 μM BSO, or, a combination of the two from 24 to 48 hpf, followed by MCB staining and imaging. 100 μM NAC significantly increased fluorescence levels across all the structures measured when compared to controls, with the greatest increases observed in the brain ventricle (312%; p < 0.0001) and the heart (240%; p < 0.0001) and the lowest increase in the yolk (52%; p < 0.0001). We chose to measure MCB fluorescence in the brain ventricle instead of the brain, due to the difficulty in distinguishing brain tissue from ventricular tissue at these earlier developmental timepoints when observed laterally [58]. Furthermore, the ventricular system is full of cerebrospinal fluid and provides the brain with all its nutrients and growth factors, along with GSH, thereby serving as a good proxy for redox changes in the brain [59]. In the zebrafish, the blood-brain barrier develops and matures only between 3 to 10 days post fertilization, and thus, compartmentalization effects were not an immediate concern for our experiments
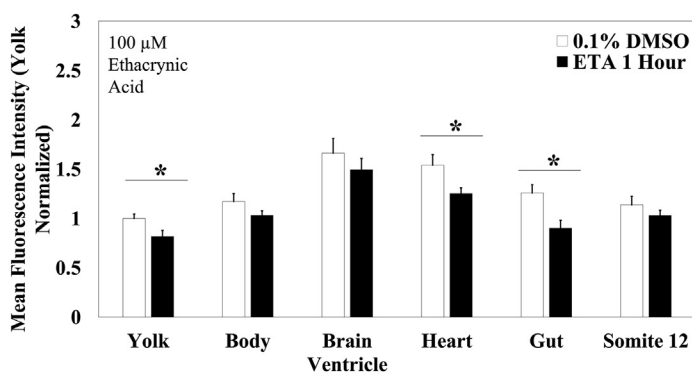
[60].

A co-treatment with 5 μM BSO abolished NAC-induced increases almost completely with all the structures showing only about a 15% increase, and the yolk showing a 6% decrease as compared to the control embryos, however, these were not significantly different from the untreated controls (Fig. 4). These data indicate a preference for glutathione as the primary thiol substrate for MCB in zebrafish embryos, as opposed to NAC. Exposure to 5 μM BSO by itself was unable to induce any statistically significant differences in fluorescence across the structures measured, but, the values showed a trend towards increased fluorescence. These data are consistent with prior studies in zebrafish embryos showing that a 24 h pretreatment with BSO is insufficient to cause glutathione depletion [52]. This could possibly be due to increased Gst expression levels following a BSO exposure. Raw fluorescence intensity values are provided in Supplementary Table T2 (Supp. Table T2).

3.4. Differential GSH depletion in the zebrafish embryo evokes commensurate responses in MCB fluorescence

We next tested the robustness of MCB staining to glutathione depletion utilizing two glutathione depleting agents – tBOOH and menadione. We treated 48 hpf zebrafish embryos with 750 μM tBOOH for 10-min or 30-min immediately prior to MCB staining. Following an acute, sub-lethal 10-min exposure to 750 μM tBOOH, zebrafish embryos showed a significant reduction in MCB fluorescence across all the structures measured (Fig. 5). Of the structures measured, the heart had the smallest decrease with only a 28% (p = 0.001) reduction and the brain ventricle had the greatest decrease with 47% (p < 0.0001) reduction in fluorescence when compared to untreated control embryos. Following a longer 30-min exposure to 750 μM tBOOH, the embryos started to return to near homeostatic conditions. All the structures measured showed an increase in MCB fluorescence. The yolk showed the greatest increase in fluorescence, gaining 45% (p < 0.0001) fluorescence followed by the brain ventricle, which gained 38% (p = 0.0028) fluorescence when compared to the 10-min exposure group. The heart, which showed the least loss of fluorescence following a 10-min exposure, also showed the smallest increase in fluorescence increasing by only 14%. All the structures returned to within 20% of their fluorescence when compared to the untreated condition.

We treated 48 hpf zebrafish embryos with 10 μM menadione for 1 h immediately prior to MCB staining and imaging. A significant decrease was measured across all structures measured; however, the fluorescence of the embryo overall did not show a significant change (Fig. 6). The brain ventricle showed the greatest reduction in fluorescence, losing around 46% (p < 0.0001) fluorescence, all the other structures showed a drop of around 30% (p < 0.0001) when compared to DMSO controls. Notably, this was different from embryos treated with tBOOH, which saw a slightly more pronounced drop in fluorescence across all
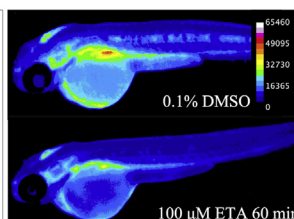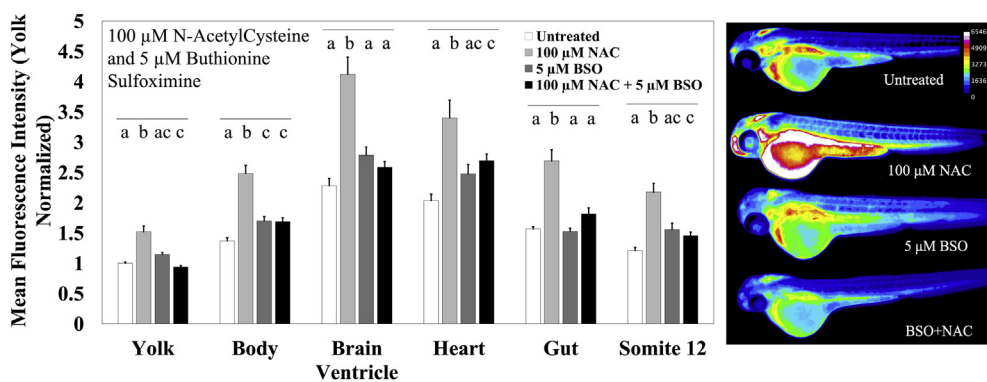

Fig. 3. GST inhibition elicits a reduction in MCB fluorescence. Zebrafish embryos aged 48 hpf were exposed to 100 μM Ethacrynic Acid for 1 h (n = 21 fish) immediately prior to MCB staining and imaging. The fluorescence intensity was compared to 0.1% DMSO treated controls (n = 24 fish). Values are mean + SEM fluorescence intensities normalized to the mean fluorescence intensity of yolk of untreated controls, combined from at least 2 independent experimental runs. Stars indicate statistically significant differences (p ≤ 0.05), as determined by a t-test across the indicated structure. Right: Heatmaps of MCB fluorescence observed in embryos exposed to the stated treatment.

Fig. 4. GSH modulation elicits a robust MCB response. Zebrafish embryos aged 48 hpf were exposed to 100 μM N-AcetylCysteine (NAC; n = 21 fish) or 5 μM Buthionine Sulfoximine (BSO; n = 28 fish), or a combination of the two (n = 40 fish) for 24 h prior to MCB staining and imaging. The fluorescence intensity was compared to untreated controls (n = 35 fish). Values are mean +SEM fluorescence intensities normalized to the mean fluorescence intensity of yolk of untreated controls, combined from at least 2 independent experimental runs. Different letters indicate statistically significant differences (p ≤ 0.05), as determined by a one-way ANOVA followed by a Tukey-Kramer post-hoc, across the indicated structure. Right: Heatmaps of monochlorobimane fluorescence observed in embryos exposed to the stated treatment.

structures following a 10 min exposure; the embryos were however able to recover fluorescence following a longer, 1 h exposure. This was in stark contrast with embryos exposed to menadione, which showed a decrease in MCB fluorescence following a 1 h exposure. This is consistent with the different mechanisms of GSH depletion employed by the two compounds: tBOOH depletes GSH by utilizing it as an electron donor during its reduction, whereas menadione directly conjugates GSH and also enters a redox cycle which continuously generates ROS leading to even greater consumption of GSH. MCB fluorescence patterns confirm this, tBOOH caused a sharp, but short-lived decrease in MCB fluorescence, whereas menadione caused a sustained decrease in MCB fluorescence.

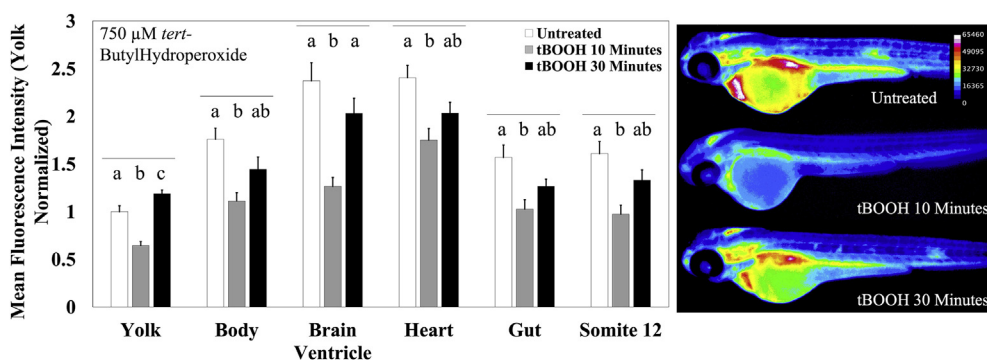### 3.5. PFOS and MEHP cause dose-specific, spatiotemporal changes in GSH utilization

In order to assess the potential of MCB as a method for detecting tissue-specific changes in GSH utilization and thus potential target organs in zebrafish embryos, we used the environmental toxicants PFOS and MEHP; we have previously characterized the effects of these chemicals on the GSH E_h in zebrafish embryos [18,54]. Embryos were exposed to either 3.2 or 32 μM PFOS from 3 hpf until either 48 or 72 hpf. At these timepoints, the embryos were stained with MCB and imaged. We saw both dose and age specific effects of PFOS exposure. At 48 hpf, a 3.2 μM exposure resulted in a significant increase of about 80% (p < 0.0001) fluorescence nearly across all structures when compared to control embryos, with the exception of the yolk, which only showed a 28% (p < 0.0001) increase. The increased fluorescence persisted at 72 hpf, with embryos showing greater nearly 150% (p < 0.0001) increase across all structures except the yolk and the gut, which showed only a 50% (p < 0.0001) increase in fluorescence (Fig. 7). In stark contrast to this, the 32 μM dose induced a decrease in fluorescence

across all the structures measured, with the most drastic decrease in the yolk and gut showing a 45% (p < 0.0001) and 60% (p < 0.0001) decrease respectively at both 48 and 72 hpf, with no overtly discernible phenotypic abnormalities (Fig. 7). These responses mirror our previous U-shaped dose response curve findings in zebrafish embryos [18,53].

Following an exposure paradigm similar to PFOS, we exposed zebrafish embryos to 200 μg/L MEHP from 3 hpf until either 48 or 72 hpf. At these timepoints, the embryos were stained with MCB and imaged. We found greater a disruption in GSH homeostasis in 48 hpf embryos, with these effects lessening by 72 hpf. At 48 hpf, the embryos showed significantly decreased MCB fluorescence; 42% (p < 0.0001) in the myotome tissue, 15% (p < 0.002) in the heart, and, 21% (p < 0.0001) in the brain ventricle (Fig. 8). These structures maintained significantly decreased fluorescence until 72 hpf, however, the fluorescence started trending towards homeostasis, with the myotome tissue showing a decrease of 24% (p < 0.0001) and the heart showing a decrease of 12% (p < 0.0001). MCB fluorescence in the brain ventricle remained low, displaying a 24% (p < 0.0001) decrease (Fig. 8). At 72 hpf, the gut showed an 18% increase in fluorescence, however, this was not statistically significant due to high variability; this variability was due to significant inter-individual differences in the autofluorescence values of the gut (Supp. Fig. S4).

4. Discussion

In this study, we present MCB staining of live zebrafish embryos as a technique to monitor glutathione redox dynamics during vertebrate embryonic development. We validated the responsiveness of MCB using well-characterized GSH modulators, and found it to be suitably sensitive to detect changes in GSH localization *in vivo*. During development, GSH utilization hotspots correlated closely with regions of high differentiation; these hotspots were differentially affected by GSH

Fig. 5. MCB responds robustly to peroxide mediated GSH depletion. Zebrafish embryos aged 48 hpf were exposed to 750 μM *tert*-Butylhydroperoxide for 10 (n = 26 fish) or 30 (n = 25 fish) minutes immediately prior to MCB staining and imaging. The fluorescence intensity was compared to untreated controls (n = 27 fish). Values are mean +SEM fluorescence intensities normalized to the mean fluorescence intensity of yolk of untreated controls, combined from at least 2 independent experimental runs. Different letters indicate statistically significant differences (p ≤ 0.05), as determined by a one-way ANOVA followed by a Tukey-Kramer post-hoc, across the indicated structure. Right: Heatmaps of MCB fluorescence observed in embryos exposed to the stated treatment.
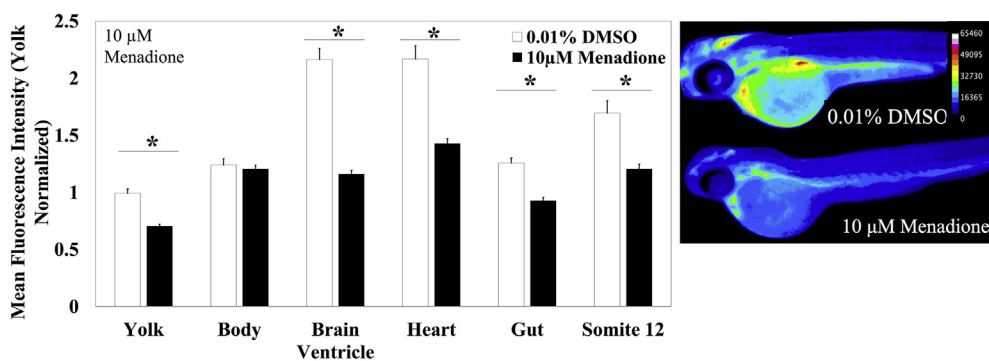
Fig. 6. MCB responds robustly to menadione induced GSH depletion. Zebrafish embryos aged 48 hpf were exposed to 10 μM Menadione for 1 h (n = 35 fish) immediately prior to MCB staining and imaging. The fluorescence intensity was compared to 0.01% DMSO controls (n = 24 fish). Values are mean +SEM fluorescence intensities normalized to the mean fluorescence intensity of yolk of untreated controls, combined from at least 2 independent experimental runs. Stars indicate statistically significant differences (p ≤ 0.05), as determined by a two-tailed *t*-test, across the indicated structure. Right: Heatmaps of monochlorobimane fluorescence observed in embryos exposed to the stated treatment.

modulation. Some organs like the heart and brain displayed a greater resiliency against GSH depletion, while the gut was especially vulnerable to GSH modulation. When applied to test the effects of PFOS exposure on embryonic GSH homeostasis, MCB was able to discern bi-directional changes in GSH utilization effected by different doses of PFOS at distinct developmental timepoints, corroborating experimentally determined GSH concentrations and the GSH E_h in the zebrafish embryo [18].

4.1. Changes in GSH utilization correspond to key developmental events

The Gst superfamily enzymes primarily function as detoxification enzymes, and are highly evolutionarily conserved [25,61]. In the zebrafish, Gst enzymes follow expression patterns similar to those seen in humans; this is true at both transcriptomic and proteomic levels [24,49,62,63]. MCB fluorescence patterns during embryonic development mirror Gst expression and embryonic GSH levels, and, correlate with key developmental events. At 24 hpf, during early organogenesis, the fluorescence levels across all structures measured were high, with the heart showing the highest fluorescence (Fig. 2). The zebrafish heart is the first mesoderm-derived organ to form, it starts differentiating and

is a linear cardiac tube at 24 hpf; by 48 hpf the heart has formed the atrium and ventricle, and, heart differentiation is complete by 72 hpf [64,65]. The heart displayed its lowest fluorescence at 48 hpf, we also saw a decrease in fluorescence across all structures measured at this developmental timepoint (Fig. 2). Of the timepoints we studied, 48 hpf is known to have the most oxidized GSH E_h, and, it is also when many of the Gst isozyme expression levels are at their lowest [24,33].

The heart and brain displayed significantly higher fluorescence levels at later timepoints, with the brain displaying the highest fluorescence at 96 hpf (Fig. 2). Of the 17 characterized zebrafish Gst isoforms the zebrafish brain predominantly expresses Gstμ1 and 2, Gstπ2 and Gsto1 [24]. With the exception of Gsto1, all these isoforms are known to be highly expressed during zebrafish embryonic development at both the protein [24] and the mRNA level [33,62,63]. Gstμ1 and 2 and Gstπ1 and 2 especially show significantly increased protein expression levels at 72 and 96 hpf, likely causing the sustained fluorescence increase in the brain [24]. Worth noting here – the heart, brain and brainstem of a 13 week old human fetus have also been reported to have high levels of cytosolic GSH, and, high Gstπ1 and Gstμ1 activities [66]. While it is difficult to make a direct comparison, at 13 weeks, most of the endoderm derived organs have patterned and differentiated,
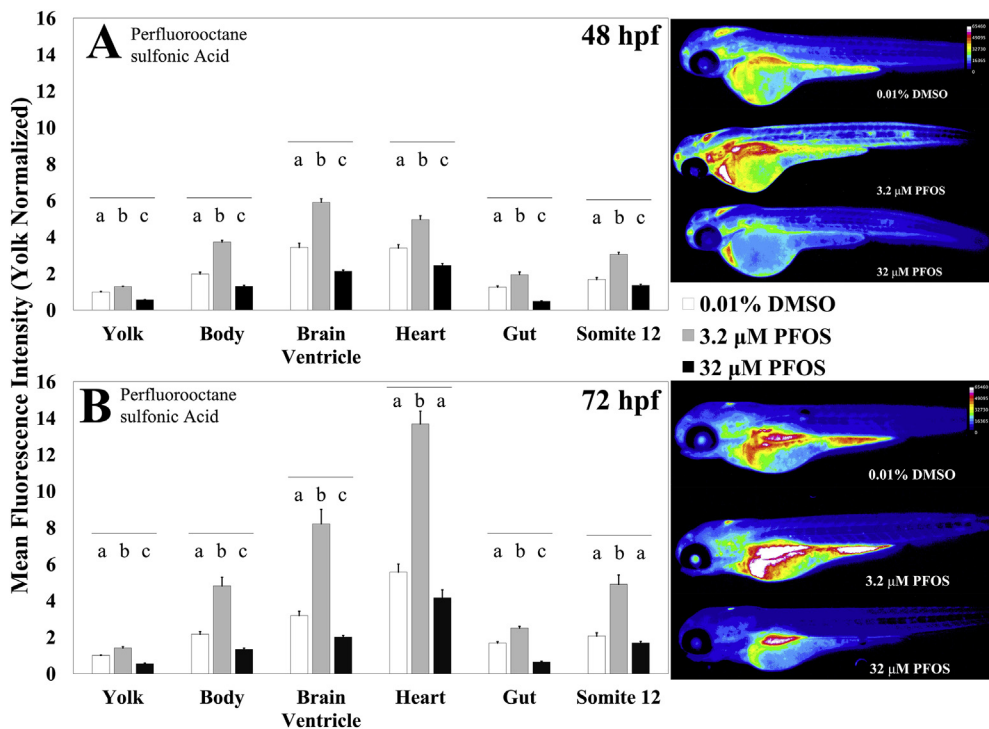

Fig. 7. Developmental PFOS exposure induces dose and structure dependent changes in MCB fluorescence. (A) Zebrafish embryos aged 48 hpf were exposed to 3.2 μM (n = 31 fish) or 32 μM (n = 31 fish) Perfluorooctane sulfonic acid (PFOS) from 3 hpf until MCB staining and imaging. The fluorescence intensity was compared to 0.01% DMSO treated controls (n = 35 fish). (B) Zebrafish embryos aged 72 hpf were exposed to 3.2 μM (n = 32) or 32 μM PFOS (n = 35 fish) from 3 hpf until MCB staining and imaging. Fluorescence intensity was compared to 0.01% DMSO treated controls (n = 35 fish). Values are mean +SEM fluorescence intensities normalized to the mean fluorescence intensity of yolk of untreated controls, combined from at least 2 independent experimental runs. Different letters indicate statistically significant differences (p ≤ 0.05), as determined by a one-way ANOVA followed by a Tukey-Kramer post-hoc, across the indicated structure. Right: Heatmaps of MCB fluorescence observed in embryos exposed to the stated treatment.
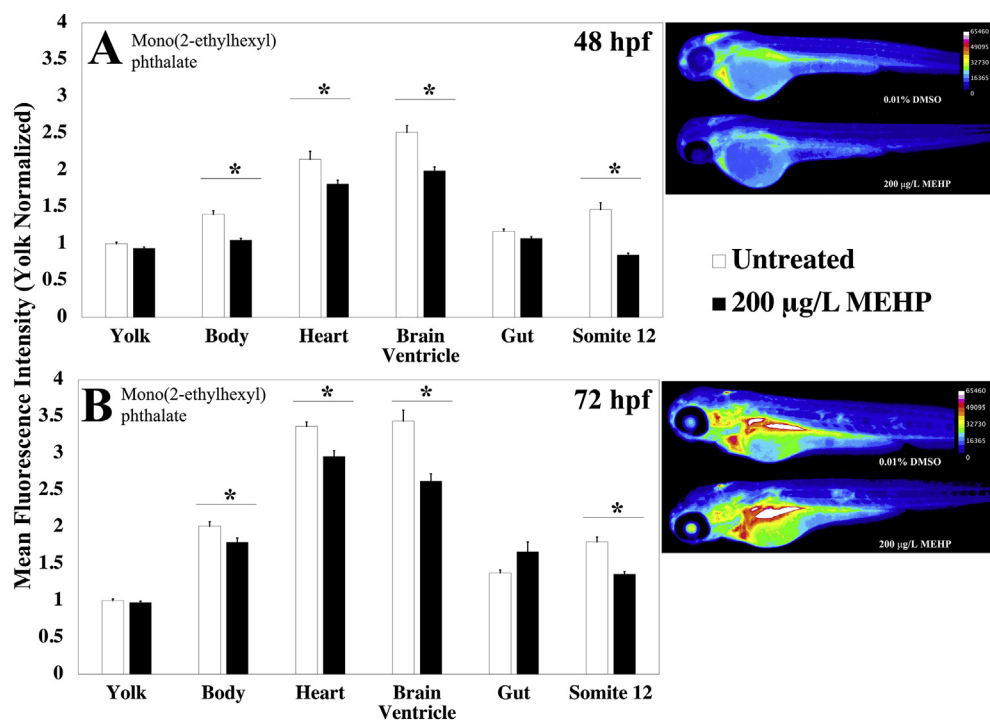
Fig. 8. Developmental MEHP exposure induces structure and age dependent changes in MCB fluorescence. (A) Zebrafish embryos aged 48 hpf were exposed to 200 µg/L Mono(2-ethylhexyl) phthalate (MEHP) (n = 34 fish) or 0.01% DMSO (n = 23 fish) from 3 hpf until MCB staining and imaging. (B) Zebrafish embryos aged 72 hpf were exposed to 200 µg/L MEHP (n = 30 fish) or 0.01% DMSO (n = 24 fish) from 3 hpf until MCB staining and imaging. Values are mean +SEM fluorescence intensities normalized to the mean fluorescence intensity of yolk of untreated controls, combined from at least 2 independent experimental runs. Stars indicate statistically significant differences (p ≤ 0.05), as determined by a t-test, across the indicated structure. Right: Heatmaps of MCB fluorescence observed in embryos exposed to the stated treatment.

approximately corresponding to 96 hpf zebrafish embryos.

The zebrafish liver bud is formed around 48 hpf, with the liver lobes growing completely by 120 hpf [67,68]. The zebrafish liver, being the primary site of Phase II metabolism, has a very high expression of all the Gst isoforms [24]. Additionally, the liver is also a major site of glutathione biosynthesis, and, is reported to have high levels of GSH in adult zebrafish [24,33]. Unsurprisingly, we found high MCB fluorescence in the developing liver at both 72 and 96 hpf, the only organs with higher levels of fluorescence were the heart and brain (Fig. 2). These data reflect reported GSH levels in human embryos and fetuses [66]. The consonance of our results with reported GSH measures across multiple vertebrate embryos (Fig. 9) confirm the high degree of evolutionary conservation of the GSH system in zebrafish, and, indicate the suitability of MCB staining to study GSH redox dynamics in zebrafish embryos [33,34,66,69–71].

4.2. GSH modulation elicits divergent responses in different organ systems during vertebrate organogenesis

The glutathione pathway has been well-studied, with the rate-limiting steps and many small-molecule inhibitors & activators well-

characterized (Fig. 1) [7]. MCB shows a robust response to modulation of the GSH pathway in zebrafish embryos. For instance, 48 hpf zebrafish embryos exposed to 750 µM tBOOH showed a reduction in MCB fluorescence following a 10 min exposure, but returned to near homeostatic conditions following a longer, 30 min exposure. These data were concordant with previous glutathione measures done using reverse-phase HPLC, where we found that 48 hpf embryos experienced a decrease in GSH and an increase in GSSG 10-min post exposure with the embryos returning to nearly homeostatic conditions after about 60 min [35]. This likely occurs due to the way living systems combat peroxide ROS, and, the short biological half-life of tBOOH [72]. Peroxides can directly oxidize sulfhydryl groups in biomolecules, however, they are quickly decomposed by cellular catalases. Given that following our tBOOH treatments, the embryos were stained for 1 h with MCB in the absence of the peroxide, the higher MCB fluorescence is potentially reflective of the ability of the embryos to buffer against, and, recover following a brief short-lived pro-oxidant insult. The additional 20 min prior to MCB exposure may have provided the embryos ample time to completely neutralize cellular tBOOH levels, and, allowed for the GSH system to start recovering. The fluorescence patterns in the gut support this interpretation, as the gut, a site of very high Gst expression does not
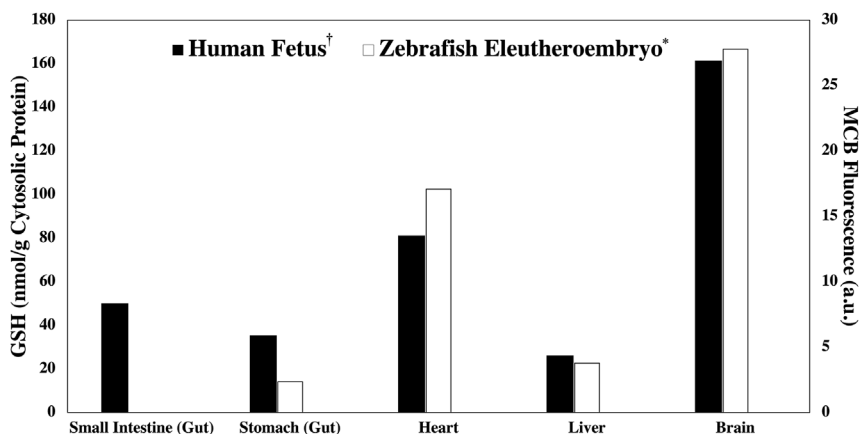

Fig. 9. MCB fluorescence patterns in the zebrafish eleutheroembryo aged 96 hpf align with known reduced GSH concentrations in a 13-week old human fetus. † Indicates data from Raijmakers et al., 2001 [66]. * Indicates data from Fig. 2; in the zebrafish eleutheroembryo, it was not possible to distinguish the stomach from the small intestine.

recover as well as some of the other structures which have lower Gst expression levels.

In contrast menadione, a quinone that depletes reduced glutathione directly by conjugating GSH, and indirectly by producing ROS, caused a decrease in MCB fluorescence across the entire embryo [73,74]. While the % change is significant, this decrease is especially apparent when comparing the heatmaps of DMSO treated embryos with menadione treated embryos (Fig. 5). We observed near complete ablation of fluorescence intensity in most embryonic structures upon menadione treatment. Previously, an exposure to 10 μM menadione has been reported to significantly increase ROS levels in developing zebrafish embryos, with perturbations in endogenous ROS levels persisting at least 24 h after the menadione exposure is terminated [75].

Ethacrynic acid (ETA), a specific inhibitor of the Gst isozyme family, caused a more subtle reduction in fluorescence when compared to tBOOH and menadione, which directly deplete cellular levels of GSH (Figs. 4 and 5) [76–78]. ETA is known to be a highly effective inhibitor of multiple zebrafish Gst isozymes, with the greatest reduction of Gstπ activity [49]. The gut, a site of high GSH utilization and Gst expression, was especially sensitive to an ETA exposure, showing the greatest decrease in MCB fluorescence (Fig. 3). This is consistent with what is known about Gst expression profiles in zebrafish embryos; Gstπ and Gstμ are the most highly expressed isozymes at the 48 hpf timepoint, with the intestine being the highest site of expression for these isozymes within the animal [24]. Confirming previous findings, our data indicate the GSH specificity of MCB, and, suggest that MCB fluorescence is a valid biological reflection of changes in GSH concentration and the rate of GSH utilization in zebrafish embryos.

In literature, MCB has been reported to react with small molecular thiols other than GSH, though this arises from the divergent substrate preferences of the Gst family present in different species [79–81]. Given the high affinity for MCB observed for the zebrafish Gst isozyme family, and the overabundance of GSH in the cellular pool of reduced thiols, this was not an immediate concern for our experiments [49]. The specificity of MCB for GSH as opposed to other thiols in zebrafish is further evidenced by the fact that exposure to BSO along with NAC completely abolished the increases in fluorescence seen when the embryos were exposed to NAC alone (Fig. 6). Since NAC boosts the cellular GSH pool and BSO inhibits the synthesis of *de novo* GSH synthesis, if the increase in MCB fluorescence upon exposure to NAC was merely due to MCB binding to NAC, the co-exposure with BSO would have failed to eliminate these gains. Collectively, the robust response of MCB to glutathione modulation in zebrafish embryos points to its suitability as a method for detecting perturbations of the GSH homeostasis during embryonic development in this model system.

4.3. Monochlorobimane provides a powerful tool to observe organism level glutathione redox dynamics

Existing literature has established that the developing vertebrate embryo uses highly specific glutathione redox signaling for spatiotemporal control and organogenesis [1,28,33,34]. Utilizing reverse-phase HPLC, accurate measures of glutathione concentrations in living systems have further bolstered the hypothesis that disruptions of the glutathione potential during development can lead to adverse health outcomes later in life [21,27,82–84]. Due to its inherent nature, HPLC requires samples to be suspended in a solvent, making it impossible to glean any spatial information regarding organism level glutathione dynamics in a live embryo. MCB has previously been employed to visualize changes in glutathione utilization in early mouse embryos, however, these experiments had to be terminated well before organogenesis began [85]. By using MCB in zebrafish embryos, we were able to reliably measure changes in glutathione utilization *in situ, in vivo* with little to no disruptions of normal embryogenetic processes like organogenesis.

Given the highly specific changes seen in MCB fluorescence patterns

in different organs during development (Fig. 2), the application of MCB to identify target tissues of toxicants becomes readily apparent. To illustrate this, we exposed zebrafish embryos to PFOS and MEHP, known exogenous GSH E_h disruptors. A 200 μg/L MEHP exposure caused a reduction in MCB fluorescence in all structures measured except the yolk and gut, at both 48 hpf and 96 hpf. The decrease in fluorescence was greater at 48 hpf than at 72 hpf, with the exception of the brain ventricle, which demonstrated a sustained decrease (Fig. 8). These data are consistent with prior studies that found MEHP induces ROS and disrupts GSH homeostasis [54,86,87].

The gut showed an interesting trend, with no observable change at 48 hpf, but, an 18% increase fluorescence at 72 hpf (Fig. 8). However, this was found to be statistically insignificant due to high inter-individual variability. This variability was caused, in part, due to inconsistent autofluorescence patterns in the gut at 72 hpf, despite all the embryos being matched for age (Supp. Fig. S4). A possible reason for these inherent differences could be the development of the gut microbiome, which is known to be present and highly variable by this stage in zebrafish embryos [88,89].

The trend towards recovery as the embryos age is likely reflective of the changes in GSH related gene expression induced by MEHP; Glutathione-disulfide reductase (Gsr), the enzyme that recycles GSSG to GSH is known to be significantly upregulated by MEHP at 72 hpf, while Gstπ expression is downregulated [54]. Furthermore, the overall GSH E_h of embryos exposed to MEHP was found to be uninterrupted by MEHP at 96 hpf [54]. Thus, one possible interpretation of these data is that MEHP induces structure-specific redox disruptions that biological antioxidant defenses are able to overcome given time. This also provides an example of the need for tools to better interrogate GSH redox dynamics during different stages of embryonic development; given the highly specific GSH E_h patterns during embryogenesis, it is not hard to imagine that a disruption of redox homeostasis during critical developmental events may make an individual more susceptible to disease later in life.

We found that the developing gut and yolk, sites of high glutathione utilization, showed a reduction in fluorescence upon treatment with 32 μM PFOS. (Fig. 7). Previously, we have shown that exposure to 32 μM PFOS leads to a more oxidized glutathione pool in zebrafish embryos, with increased GSSG concentrations; we also found reduced expression of Keap1a and Keap1b, cytosolic repressors of Nrf2 [18]. We observed accelerated yolk consumption, and, aberrant pancreatic development upon PFOS exposure [18,53].

Worth noting here is that the lower dose of PFOS induced an increase in MCB fluorescence, resulting in a non-monotonic inverted "U-shaped" dose response curve. This trend has been observed previously with PFOS, and is likely owing to an adaptive response in embryos at the lower dose [18,53]. We found that a 3.2 μM PFOS exposure resulted in the brain ventricle gaining the greatest MCB fluorescence at both 48 hpf (72%) and 72 hpf (158%; Fig. 7), however, this was not accompanied by any adverse phenotypic outcomes. In the zebrafish model, a chronic larval 0.5 μM exposure to PFOS has been reported to induce later-life behavioral effects in exposed fish, and, morphological abnormalities in their offspring [90]. Furthermore, a single static exposure to 2 μM PFOS during early development (3 hpf to 120 hpf) has been reported to cause behavioral changes that persist well into adulthood, despite no apparent morphological defects; *tgfb1a* expression was found to be significantly upregulated in animals exposed to 2 μM PFOS [91].

The Tgfb1 pathway and the Keap1-Nrf2 pathway have been well-studied to identify potential crosstalk, with divergent effects seen in different cell lineages. In renal cells, overexpression of Tgfb1 has been shown to induce ROS formation, and, decrease the expression of Nrf2 and GSH synthesis genes, leading to malignant transformation; in human pancreatic ductal cells, Tgb1 was found to activate Nrf2 and GSH synthesis genes, leading to malignant transformation [92,93]. Tgfb1 is a good representative example of a transcription factor affected by disrupted GSH homeostasis, and, these data indicate the predictive

power of MCB as a technique to identify potential PFOS target organs.

The increases in MCB could arise due to increases in GSH concentrations, or, increases in GST activity. While the determination of the exact molecular mechanisms underlying PFOS toxicity, as they relate to GSH homeostasis, is outside the scope of this study, MCB could be employed in conjunction with ETA to tease apart changes in GSH concentration vs GST activity. Additionally, GSH modulators like NAC and BSO could be employed to better understand the contribution of GSH perturbations to PFOS toxicity. Thus, experiments with MCB could serve as an initial screening tool, helping discern embryonic structures adversely affected by xenobiotics; further studies could then be carried out to pinpoint exact molecular targets mediating xenobiotic toxicity.

While MCB cannot easily differentiate between changes in GSH concentration vs GSH utilization, it does provide an indiscriminate, unbiased method to investigate the differential sensitivity of organs to xenobiotic induced GSH disruptions; furthermore, it presents organ specific GSH disruptions in the context of the entire organism, as opposed to genetically encoded fluorescent redox biosensors like Grx1-roGFP2 and the RedoxFluor that look at GSH changes in a specific organ structure E_h.

A key shortcoming of MCB staining is the inability to directly translate fluorescence levels to GSH concentrations or the GSH E_h. However, this could be overcome by coupling MCB staining with redox biosensors, which can equilibrate with the intracellular pools of GSH and give a more precise quantitative estimate of the GSH E_h [94,95]. Furthermore, MCB is susceptible to some of the same challenges as other chemical GSH probes [96]. It is capable of binding to other biological thiols, albeit with less specificity than its specificity for GSH; the responsiveness of MCB is also greatly impacted by the inherent GSH concentrations and Gst expression profiles of the cell type being investigated.

Both the intracellular GSH concentrations and Gst expression profiles are known to be highly divergent across different organs, and, organisms. For instance, MCB is known to be a poor substrate for a majority of primate GST isozymes [81]. Therefore, it is necessary to characterize these factors in any model system before the application of MCB as a GSH detection tool. In the zebrafish, GSH levels are known to be in the mM range, higher than other thiols like cysteine, and, the Gst isozymes are known to utilize MCB efficiently, hence, it is well-suited for this technique [33,49]. Caution must be exercised when translating changes in MCB fluorescence to biological outcomes. Unlike more advanced imaging techniques like MALDI imaging of GSH, MCB is incapable of distinguishing between GSH and GSH conjugates derived in a thiol independent manner. MCB's utility derives from its ability to be quickly and inexpensively employed to screen perturbations in the GSH system across a whole embryo upon xenobiotic exposure.

The developing embryo is a highly organized collection of diverse populations of cells & biological matrices, all of which have divergent redox potentials [97]. This, coupled with the ever increasing number of environmental toxicants underscore the need for techniques to accurately, affordably and quickly assess interruptions in the redox microenvironment during development with minimal disruptions to normal biology. MCB staining could help bridge a gap in developmental redox biology by facilitating visualization of tissue specific changes in GSH during normal embryonic development. By enabling us to observe organism level changes in glutathione redox dynamics upon chemical exposure, it can find broad application as a tool to gauge the safety of chemicals.

5. Conclusions

This study presents a novel application of MCB as a tool to visualize glutathione redox dynamics *in vivo* during vertebrate embryonic development using the zebrafish model. GSH localization was found to be highly spatiotemporal in the developing embryo, corresponding to Gst expression patterns. MCB responded robustly to GSH modulation, with different organs displaying different sensitivities to GSH modulation. The heart and brain were found to be especially resilient to oxidizing redox disruptions. The highly specific and reproducible spatiotemporal patterns of GSH utilization are indicative of there being potential biological consequences of developmental GSH disruptions. The environmental toxicants PFOS and MEHP, exogenous disruptors of the GSH E_h, induced dose-dependent, age and structure specific changes in MCB fluorescence. Our data indicate the broad application potential of MCB as an unbiased method to assess GSH interruptions arising from chemical exposures in live embryos.

Appendix A. Supplementary data

Supplementary data to this article can be found online at https://doi.org/10.1016/j.redox.2019.101235.

References

[1] A.R. Timme-Laragy, M.E. Hahn, J.M. Hansen, A. Rastogi, M.A. Roy, Redox stress and signaling during vertebrate embryonic development: regulation and responses, Semin. Cell Dev. Biol. 80 (2018) 17–28.

[2] E. Hoarau, V. Chandra, P. Rustin, R. Scharfmann, B. Duvillie, Pro-oxidant/anti-oxidant balance controls pancreatic beta-cell differentiation through the ERK1/2 pathway, Cell Death Dis. 5 (2014) e1487.

[3] L.P. Thompson, Y. Al-Hasan, Impact of oxidative stress in fetal programming, J. Pregnancy 2012 (2012) 8.

[4] J. de Faria Poloni, H. Chapola, B.C. Feltes, D. Bonatto, The importance of sphingolipids and reactive oxygen species in cardiovascular development, Biol. Cell 106 (6) (2014) 167–181.

[5] J. Smith, E. Ladi, M. Mayer-Proschel, M. Noble, Redox state is a central modulator of the balance between self-renewal and differentiation in a dividing glial precursor cell, Proc. Natl. Acad. Sci. U. S. A. 97 (18) (2000) 10032–10037.

[6] S.C. Lu, Glutathione synthesis, Biochim. Biophys. Acta 1830 (5) (2013) 3143–3153.

[7] S.C. Lu, Regulation of glutathione synthesis, Mol. Asp. Med. 30 (1–2) (2009) 42–59.

[8] D.P. Jones, Redefining oxidative stress, Antioxidants Redox Signal. 8 (9–10) (2006) 1865–1879.

[9] F.Q. Schafer, G.R. Buettner, Redox environment of the cell as viewed through the redox state of the glutathione disulfide/glutathione couple, Free Radic. Biol. Med. 30 (11) (2001) 1191–1212.

[10] L. Liu, D.L. Keefe, Cytoplasm mediates both development and oxidation-induced apoptotic cell death in mouse zygotes, Biol. Reprod. 62 (6) (2000) 1828–1834.

[11] E. Salas-Vidal, H. Lomeli, S. Castro-Obregon, R. Cuervo, D. Escalante-Alcalde, L. Covarrubias, Reactive oxygen species participate in the control of mouse embryonic cell death, Exp. Cell Res. 238 (1) (1998) 136–147.

[12] J.A. Coffman, A. Coluccio, A. Planchart, A.J. Robertson, Oral-aboral axis specification in the sea urchin embryo III. Role of mitochondrial redox signaling via H2O2, Dev. Biol. 330 (1) (2009) 123–130.

[13] W.G. Kirlin, J. Cai, S.A. Thompson, D. Diaz, T.J. Kavanagh, D.P. Jones, Glutathione redox potential in response to differentiation and enzyme inducers, Free Radic. Biol. Med. 27 (11–12) (1999) 1208–1218.

[14] Y.S. Nkabyo, T.R. Ziegler, L.H. Gu, W.H. Watson, D.P. Jones, Glutathione and thioredoxin redox during differentiation in human colon epithelial (Caco-2) cells, Am. J. Physiol. Gastrointest. Liver Physiol. 283 (6) (2002) G1352–G1359.

[15] D.P. Jones, Redox potential of GSH/GSSG couple: assay and biological significance, Methods Enzymol. 348 (2002) 93–112.

[16] P.D. Ray, B.W. Huang, Y. Tsuji, Reactive oxygen species (ROS) homeostasis and redox regulation in cellular signaling, Cell. Signal. 24 (5) (2012) 981–990.

[17] G.M. Cohen, M. d'Arcy Doherty, Free radical mediated cell toxicity by redox cycling chemicals, Br. J. Canc. Suppl. 8 (1987) 46–52.

[18] K.E. Sant, P.P. Sinno, H.M. Jacobs, A.R. Timme-Laragy, Nrf2a modulates the embryonic antioxidant response to perfluorooctanesulfonic acid (PFOS) in the zebrafish, Danio rerio, Aquat. Toxicol. 198 (2018) 92–102.

[19] R.F. Leite, K. Annes, J. Ispada, C.B. de Lima, E.C. Dos Santos, P.K. Fontes, M.F.G. Nogueira, M.P. Milazzotto, Oxidative stress alters the profile of transcription factors related to early development on in vitro produced embryos, Oxidative Med. Cell. Longev. 2017 (2017) 1502489.

[20] M.E. Rousseau, K.E. Sant, L.R. Borden, D.G. Franks, M.E. Hahn, A.R. Timme-Laragy, Regulation of Ahr signaling by Nrf2 during development: effects of Nrf2a deficiency on PCB126 embryotoxicity in zebrafish (Danio rerio), Aquat. Toxicol. 167 (2015) 157–171.

[21] J.M. Hansen, C. Harris, Redox control of teratogenesis, Reprod. Toxicol. 35 (2013) 165–179.

[22] C. Harris, J.M. Hansen, Nrf2-mediated resistance to oxidant-induced redox disruption in embryos, Birth Defects Res. Part B Dev. Reproductive Toxicol. 95 (3) (2012) 213–218.

[23] Q. Ma, Role of nrf2 in oxidative stress and toxicity, Annu. Rev. Pharmacol. Toxicol. 53 (2013) 401–426.

[24] A. Tierbach, K.J. Groh, R. Schonenberger, K. Schirmer, M.J. Suter, Glutathione S-transferase protein expression in different life stages of zebrafish (Danio rerio), Toxicol. Sci. 162 (2) (2018) 702–712.

[25] J.D. Hayes, D.J. Pulford, The glutathione S-transferase supergene family: regulation of GST and the contribution of the isoenzymes to cancer chemoprotection and drug resistance, Crit. Rev. Biochem. Mol. Biol. 30 (6) (1995) 445–600.

[26] S. Landi, Mammalian class theta GST and differential susceptibility to carcinogens: a review, Mutat. Res. 463 (3) (2000) 247–283.

[27] J.M. Hansen, Oxidative stress as a mechanism of teratogenesis, Birth Defects Res. Part C Embryo Today - Rev. 78 (4) (2006) 293–307.

[28] C. Harris, D.Z. Shuster, R. Roman Gomez, K.E. Sant, M.S. Reed, J. Pohl, J.M. Hansen, Inhibition of glutathione biosynthesis alters compartmental redox status and the thiol proteome in organogenesis-stage rat conceptuses, Free Radic. Biol. Med. 63 (2013) 325–337.

[29] R. Meunier, Stages in the development of a model organism as a platform for mechanistic models in developmental biology: zebrafish, 1970-2000, Stud. Hist. Philos. Sci. C Stud. Hist. Philos. Biol. Biomed. Sci. 43 (2) (2012) 522–531.

[30] M.B. Veldman, S. Lin, Zebrafish as a developmental model organism for pediatric research, Pediatr. Res. 64 (5) (2008) 470–476.

[31] A.J. Hill, H. Teraoka, W. Heideman, R.E. Peterson, Zebrafish as a model vertebrate for investigating chemical toxicity, Toxicol. Sci. 86 (1) (2005) 6–19.

[32] Y.J. Dai, Y.F. Jia, N. Chen, W.P. Bian, Q.K. Li, Y.B. Ma, Y.L. Chen, D.S. Pei, Zebrafish as a model system to study toxicology, Environ. Toxicol. Chem. 33 (1) (2014) 11–17.

[33] A.R. Timme-Laragy, J.V. Goldstone, B.R. Imhoff, J.J. Stegeman, M.E. Hahn, J.M. Hansen, Glutathione redox dynamics and expression of glutathione-related genes in the developing embryo, Free Radic. Biol. Med. 65 (2013) 89–101.

[34] J.M. Hansen, C. Harris, Glutathione during embryonic development, Biochim. Biophys. Acta 1850 (8) (2015) 1527–1542.

[35] K.E. Sant, J.M. Hansen, L.M. Williams, N.L. Tran, J.V. Goldstone, J.J. Stegeman, M.E. Hahn, A. Timme-Laragy, The role of Nrf1 and Nrf2 in the regulation of glutathione and redox dynamics in the developing zebrafish embryo, Redox Biol. 13 (2017) 207–218.

[36] Z.Z. Shi, J. Osei-Frimpong, G. Kala, S.V. Kala, R.J. Barrios, G.M. Habib, D.J. Lukin, C.M. Danney, M.M. Matzuk, M.W. Lieberman, Glutathione synthesis is essential for mouse development but not for cell growth in culture, Proc. Natl. Acad. Sci. U. S. A. 97 (10) (2000) 5101–5106.

[37] Y. Will, K.A. Fischer, R.A. Horton, R.S. Kaetzel, M.K. Brown, O. Hedstrom, M.W. Lieberman, D.J. Reed, gamma-glutamyltranspeptidase-deficient knockout mice as a model to study the relationship between glutathione status, mitochondrial function, and cellular function, Hepatology 32 (4 Pt 1) (2000) 740–749.

[38] L. Swain, M.S. Nanadikar, S. Borowik, A. Zieseniss, D.M. Katschinski, Transgenic organisms meet redox bioimaging: one step closer to physiology, Antioxidants Redox Signal. 29 (6) (2018) 603–612.

[39] X. Zhao, K. Lorent, B.J. Wilkins, D.M. Marchione, K. Gillespie, O. Waisbourd-Zinman, J. So, K.A. Koo, D. Shin, J.R. Porter, R.G. Wells, I. Blair, M. Pack, Glutathione antioxidant pathway activity and reserve determine toxicity and specificity of the biliary toxin biliatresone in zebrafish, Hepatology 64 (3) (2016) 894–907.

[40] E. Panieri, C. Millia, M.M. Santoro, Real-time quantification of subcellular H2O2 and glutathione redox potential in living cardiovascular tissues, Free Radic. Biol. Med. 109 (2017) 189–200.

[41] B. Kalyanaraman, V. Darley-Usmar, K.J. Davies, P.A. Dennery, H.J. Forman, M.B. Grisham, G.E. Mann, K. Moore, L.J. Roberts 2nd, H. Ischiropoulos, Measuring reactive oxygen and nitrogen species with fluorescent probes: challenges and limitations, Free Radic. Biol. Med. 52 (1) (2012) 1–6.

[42] H. Kamencic, A. Lyon, P.G. Paterson, B.H. Juurlink, Monochlorobimane fluorometric method to measure tissue glutathione, Anal. Biochem. 286 (1) (2000) 35–37.

[43] T. Lorincz, A. Szarka, The determination of hepatic glutathione at tissue and subcellular level, J. Pharmacol. Toxicol. Methods 88 (Pt 1) (2017) 32–39.

[44] S. Keshavarzi, M. Salehi, F. Farifteh-Nobijari, T. Hosseini, S. Hosseini, A. Ghazifard, M. Ghaffari Novin, V. Fallah-Omrani, A. Nourozian, A. Hosseini, Melatonin modifies histone acetylation during in vitro maturation of mouse oocytes, Cell J 20 (2) (2018) 244–249.

[45] M. Narasimhan, M. Rathinam, D. Patel, G. Henderson, L. Mahimainathan, Astrocytes prevent ethanol induced apoptosis of Nrf2 depleted neurons by maintaining GSH homeostasis, Open J. Apoptosis 1 (2) (2012).

[46] G. Bellomo, M. Vairetti, L. Stivala, F. Mirabelli, P. Richelmi, S. Orrenius, Demonstration of nuclear compartmentalization of glutathione in hepatocytes, Proc. Natl. Acad. Sci. U. S. A. 89 (10) (1992) 4412–4416.

[47] A. Jos, A.M. Camean, S. Pflugmacher, H. Segner, The antioxidant glutathione in the fish cell lines EPC and BCF-2: response to model pro-oxidants as measured by three different fluorescent dyes, Toxicol. Vitro 23 (3) (2009) 546–553.

[48] J. Sebastia, R. Cristofol, M. Martin, E. Rodriguez-Farre, C. Sanfeliu, Evaluation of fluorescent dyes for measuring intracellular glutathione content in primary cultures

[49] of human neurons and neuroblastoma SH-SY5Y, Cytometry 51 (1) (2003) 16–25.

[49] B. Glisic, I. Mihaljevic, M. Popovic, R. Zaja, J. Loncar, K. Fent, R. Kovacevic, T. Smital, Characterization of glutathione-S-transferases in zebrafish (Danio rerio), Aquat. Toxicol. 158 (2015) 50–62.

[50] C.B. Kimmel, W.W. Ballard, S.R. Kimmel, B. Ullmann, T.F. Schilling, Stages of embryonic development of the zebrafish, Dev. Dynam. 203 (3) (1995) 253–310.

[51] C.Y. Usenko, S.L. Harper, R.L. Tanguay, Fullerene C60 exposure elicits an oxidative stress response in embryonic zebrafish, Toxicol. Appl. Pharmacol. 229 (1) (2008) 44–55.

[52] A.R. Timme-Laragy, L.A. Van Tiem, E.A. Linney, R.T. Di Giulio, Antioxidant responses and NRF2 in synergistic developmental toxicity of PAHs in zebrafish, Toxicol. Sci. 109 (2) (2009) 217–227.

[53] K.E. Sant, H.M. Jacobs, K.A. Borofski, J.B. Moss, A.R. Timme-Laragy, Embryonic exposures to perfluorooctanesulfonic acid (PFOS) disrupt pancreatic organogenesis in the zebrafish, Danio rerio, Environ. Pollut. 220 (Pt B) (2017) 807–817.

[54] H.M. Jacobs, K.E. Sant, A. Basnet, L.M. Williams, J.B. Moss, A.R. Timme-Laragy, Embryonic exposure to Mono(2-ethylhexyl) phthalate (MEHP) disrupts pancreatic organogenesis in zebrafish (Danio rerio), Chemosphere 195 (2018) 498–507.

[55] W. Zhai, Z. Huang, L. Chen, C. Feng, B. Li, T. Li, Thyroid endocrine disruption in zebrafish larvae after exposure to mono-(2-ethylhexyl) phthalate (MEHP), PLoS One 9 (3) (2014) e92465.

[56] A. Gorlach, K. Bertram, S. Hudecova, O. Krizanova, Calcium and ROS: a mutual interplay, Redox Biol. 6 (2015) 260–271.

[57] OECD, Test No 236, Fish Embryo Acute Toxicity (FET) Test, (2013).

[58] V. Korzh, Development of brain ventricular system, Cell. Mol. Life Sci. 75 (3) (2018) 375–383.

[59] M. Samuelsson, L. Vainikka, K. Ollinger, Glutathione in the blood and cerebrospinal fluid: a study in healthy male volunteers, Neuropeptides 45 (4) (2011) 287–292.

[60] A. Fleming, H. Diekmann, P. Goldsmith, Functional characterisation of the maturation of the blood-brain barrier in larval zebrafish, PLoS One 8 (10) (2013) e77548.

[61] D. Sheehan, G. Meade, V.M. Foley, C.A. Dowd, Structure, function and evolution of glutathione transferases: implications for classification of non-mammalian members of an ancient enzyme superfamily, Biochem. J. 360 (Pt 1) (2001) 1–16.

[62] B. Glisic, J. Hrubik, S. Fa, N. Dopudj, R. Kovacevic, N. Andric, Transcriptional profiles of glutathione-S-Transferase isoforms, Cyp, and AOE genes in atrazine-exposed zebrafish embryos, Environ. Toxicol. 31 (2) (2016) 233–244.

[63] M.S. Abunnaja, K. Kurogi, Y.I. Mohammed, Y. Sakakibara, M. Suiko, E.A. Hassoun, M.C. Liu, Identification and characterization of the zebrafish glutathione S-transferase Pi-1, J. Biochem. Mol. Toxicol. 31 (10) (2017).

[64] J. Bakkers, Zebrafish as a model to study cardiac development and human cardiac disease, Cardiovasc. Res. 91 (2) (2011) 279–288.

[65] D.Y. Stainier, R.K. Lee, M.C. Fishman, Cardiovascular development in the zebrafish. I. Myocardial fate map and heart tube formation, Development 119 (1) (1993) 31–40.

[66] M.T. Raijmakers, E.A. Steegers, W.H. Peters, Glutathione S-transferases and thiol concentrations in embryonic and early fetal tissues, Hum. Reprod. 16 (11) (2001) 2445–2450.

[67] J. Chu, K.C. Sadler, New school in liver development: lessons from zebrafish, Hepatology 50 (5) (2009) 1656–1663.

[68] B.J. Wilkins, M. Pack, Zebrafish models of human liver development and disease, Comp. Physiol. 3 (3) (2013) 1213–1230.

[69] C. Ufer, C.C. Wang, The roles of glutathione peroxidases during embryo development, Front. Mol. Neurosci. 4 (2011) 12.

[70] C.S. Gardiner, D.J. Reed, Synthesis of glutathione in the preimplantation mouse embryo, Arch. Biochem. Biophys. 318 (1) (1995) 30–36.

[71] C.S. Gardiner, D.J. Reed, Status of glutathione during oxidant-induced oxidative stress in the preimplantation mouse embryo, Biol. Reprod. 51 (6) (1994) 1307–1314.

[72] R. Dringen, L. Kussmaul, B. Hamprecht, Detoxification of exogenous hydrogen peroxide and organic hydroperoxides by cultured astroglial cells assessed by microtiter plate assay, Brain Res. Protoc. 2 (3) (1998) 223–228.

[73] D. Ross, H. Thor, S. Orrenius, P. Moldeus, Interaction of menadione (2-methyl-1,4-naphthoquinone) with glutathione, Chem. Biol. Interact. 55 (1–2) (1985) 177–184.

[74] T.J. Chiou, W.F. Tzeng, The roles of glutathione and antioxidant enzymes in menadione-induced oxidative stress, Toxicology 154 (1–3) (2000) 75–84.

[75] C.L. Bladen, D.J. Kozlowski, W.S. Dynan, Effects of low-dose ionizing radiation and menadione, an inducer of oxidative stress, alone and in combination in a vertebrate embryo model, Radiat. Res. 178 (5) (2012) 499–503.

[76] S. Awasthi, S.K. Srivastava, F. Ahmad, H. Ahmad, G.A. Ansari, Interactions of glutathione S-transferase-pi with ethacrynic acid and its glutathione conjugate, Biochim. Biophys. Acta 1164 (2) (1993) 173–178.

[77] J.H. Ploemen, B. van Ommen, J.J. Bogaards, P.J. van Bladeren, Ethacrynic acid and its glutathione conjugate as inhibitors of glutathione S-transferases, Xenobiotica 23 (8) (1993) 913–923.

[78] J.H. Ploemen, J.J. Bogaards, G.A. Veldink, B. van Ommen, D.H. Jansen, P.J. van Bladeren, Isoenzyme selective irreversible inhibition of rat and human glutathione S-transferases by ethacrynic acid and two brominated derivatives, Biochem. Pharmacol. 45 (3) (1993) 633–639.

[79] D.W. Hedley, S. Chow, Evaluation of methods for measuring cellular glutathione content using flow cytometry, Cytometry 15 (4) (1994) 349–358.

[80] G.C. Rice, E.A. Bump, D.C. Shrieve, W. Lee, M. Kovacs, Quantitative analysis of cellular glutathione by flow cytometry utilizing monochlorobimane: some applications to radiation and drug resistance in vitro and in vivo, Cancer Res. 46 (12 Pt 1) (1986) 6105–6110.

[81] G.A. Ublacker, J.A. Johnson, F.L. Siegel, R.T. Mulcahy, Influence of glutathione S-

transferases on cellular glutathione determination by flow cytometry using mono-chlorobimane, Cancer Res. 51 (7) (1991) 1783–1788.

[82] J.M. Hansen, E.W. Carney, C. Harris, Differential alteration by thalidomide of the glutathione content of rat vs. rabbit conceptuses in vitro, Reprod. Toxicol. 13 (6) (1999) 547–554.

[83] J.M. Hansen, C. Harris, A novel hypothesis for thalidomide-induced limb teratogenesis: redox misregulation of the NF-kappaB pathway, Antioxidants Redox Signal. 6 (1) (2004) 1–14.

[84] D.J. Barker, C. Osmond, Infant mortality, childhood nutrition, and ischaemic heart disease in England and Wales, Lancet 1 (8489) (1986) 1077–1081.

[85] R. Dumollard, Z. Ward, J. Carroll, M.R. Duchen, Regulation of redox metabolism in the mouse oocyte and embryo, Development 134 (3) (2007) 455–465.

[86] N. Liu, L. Jiang, X. Sun, X. Yao, X. Zhai, X. Liu, X. Wu, Y. Bai, S. Wang, G. Yang, Mono-(2-ethylhexyl) phthalate induced ROS-dependent autophagic cell death in human vascular endothelial cells, Toxicol. Vitro 44 (2017) 49–56.

[87] W. Wang, Z.R. Craig, M.S. Basavarajappa, K.S. Hafner, J.A. Flaws, Mono-(2-ethyl-hexyl) phthalate induces oxidative stress and inhibits growth of mouse ovarian antral follicles, Biol. Reprod. 87 (6) (2012) 152.

[88] G. Roeselers, E.K. Mittge, W.Z. Stephens, D.M. Parichy, C.M. Cavanaugh, K. Guillemin, J.F. Rawls, Evidence for a core gut microbiota in the zebrafish, ISME J. 5 (10) (2011) 1595–1608.

[89] W.Z. Stephens, A.R. Burns, K. Stagaman, S. Wong, J.F. Rawls, K. Guillemin, B.J. Bohannan, The composition of the zebrafish intestinal microbial community varies across development, ISME J. 10 (3) (2016) 644–654.

[90] J. Chen, S.R. Das, J. La Du, M.M. Corvi, C. Bai, Y. Chen, X. Liu, G. Zhu, R.L. Tanguay, Q. Dong, C. Huang, Chronic PFOS exposures induce life stage-specific behavioral deficits in adult zebrafish and produce malformation and behavioral deficits in F1 offspring, Environ. Toxicol. Chem. 32 (1) (2013) 201–206.

[91] C.E. Jantzen, K.M. Annunziato, K.R. Cooper, Behavioral, morphometric, and gene expression effects in adult zebrafish (Danio rerio) embryonically exposed to PFOA, PFOS, and PFNA, Aquat. Toxicol. 180 (2016) 123–130.

[92] I.G. Ryoo, H. Ha, M.K. Kwak, Inhibitory role of the KEAP1-NRF2 pathway in TGFbeta1-stimulated renal epithelial transition to fibroblastic cells: a modulatory effect on SMAD signaling, PLoS One 9 (4) (2014) e93265.

[93] S. Arfmann-Knubel, B. Struck, G. Genrich, O. Helm, B. Sipos, S. Sebens, H. Schafer, The crosstalk between Nrf2 and TGF-beta1 in the epithelial-mesenchymal transition of pancreatic duct epithelial cells, PLoS One 10 (7) (2015) e0132978.

[94] T. Yano, M. Oku, N. Akeyama, A. Itoyama, H. Yurimoto, S. Kuge, Y. Fujiki, Y. Sakai, A novel fluorescent sensor protein for visualization of redox states in the cytoplasm and in peroxisomes, Mol. Cell. Biol. 30 (15) (2010) 3758–3766.

[95] M. Gutscher, A.L. Pauleau, L. Marty, T. Brach, G.H. Wabnitz, Y. Samstag, A.J. Meyer, T.P. Dick, Real-time imaging of the intracellular glutathione redox potential, Nat. Methods 5 (6) (2008) 553–559.

[96] C. Cossetti, G. Di Giovamberardino, R. Rota, A. Pastore, Pitfalls in the quantitative imaging of glutathione in living cells, Nat. Commun. 9 (1) (2018) 1588.

[97] D.P. Jones, Y. Liang, Measuring the poise of thiol/disulfide couples in vivo, Free Radic. Biol. Med. 47 (10) (2009) 1329–1338.